Journal of
Mechanical
Science and
Technology

Journal of Mechanical Science and Technology 21 (2007) 1344~1351

A Gas-kinetic Discontinuous Galerkin Method for Viscous Flow Equations

Hongwei Liu*, Kun Xu

Department of Mathematics, Hong Kong University of Science and Technology, Kowloon, Hong Kong

(Manuscript Received December 21, 2006; Revised March 2, 2007; Accepted May 2, 2007)

Abstract

This paper presents a Runge-Kutta discontinuous Galerkin (RKDG) method for viscous flow computation. The construction of the RKDG method is based on a gas-kinetic formulation, which not only couples the convective and dissipative terms together, but also includes both discontinuous and continuous representation in the flux evaluation at the cell interface through a simple hybrid gas distribution function. Due to the intrinsic connection between the gas-kinetic BGK model and the Navier-Stokes equations, the Navier-Stokes flux is automatically obtained by the present method. Numerical examples for both one dimensional (1D) and two dimensional (2D) compressible viscous flows are presented to demonstrate the accuracy and shock capturing capability of the current RKDG method.

Keywords: RKDG method; Gas-kinetic scheme; Navier-stokes equations

1. Introduction

In the past decades, both the finite volume (FV) and the discontinuous Galerkin (DG) finite element methods have been successfully developed for the compressible flow simulations. Most FV schemes use piecewise constant representation for the flow variables and employ the reconstruction techniques to obtain high accuracy. A higher-order scheme usually has a larger stencil than a lower-order scheme, which makes it difficult to be applied on unstructured mesh or complicated geometry. For the DG method high-order accuracy is obtained by means of high-order approximation within each element, where more information is stored for each element during the computation. The compactness of the DG method allows it to deal with unstructured mesh or complicated geometry easily. Now the DG method has served as a high-order method for a broad class of engineering problems (Cockburn et al., 2000).

For viscous flow problems, many successful DG methods have been proposed in the literature, such as those by Bassi and Rebay (1997), Cockburn and Shu (1998), Baumann and Oden (1999), and many others. In Arnold et al. (2002), a large class of discontinuous Galerkin methods for second-order elliptic problems have been analyzed in a unified framework. More recently, van Leer and Nomura (2005) proposed a recovery-based DG method for diffusion equation using the recovery principle. This method has deep physical insight in the construction of a DG method for convection-diffusion problem.

The RKDG method for non-linear convection-dominated problems was first proposed and studied by Cockburn and his collaborators in a series of papers (Cockburn et al., 1989a; 1989b; 1990; 1998; 1998), see Cockburn et al. (2001) for a review of the method. The excellent results obtained by the high-order accurate RKDG method demonstrated itself as a powerful tool in the computational fluid dynamics.

*Corresponding author. Tel.: +852 2358 7453, Fax.: +852 2358 1643
E-mail address: hwliu@ust.hk

Recently, the gas-kinetic RKDG method proposed by Tang and Warnecke (2005) has been shown to be very accurate and efficient for inviscid flow simulations.

In this paper, a RKDG method for the viscous flow problems based on a gas-kinetic formulation will be presented. Instead of treating the convection and dissipation effects separately, we use the gas-kinetic distribution function with both inviscid and viscous terms in the construction of the numerical flux at the cell interface. Due to the intrinsic connection between the gas-kinetic BGK model and the Navier-Stokes equations, the Navier-Stokes flux is automatically obtained by the RKDG method. The numerical dissipation introduced from the discontinuity at the cell interface is favored by the inviscid flow calculation, especially for the capturing of numerical shock fronts. For viscous flow problems, it should be avoided because the artificial viscosity from the discontinuity deteriorates the physical one Xu (2001). A simplified gas-kinetic relaxation model, which plays the role of recovering the continuity of the flow variables from the initial discontinuous representation, will be used in the present method. In Xu (2004), the DG-BGK method has been developed which gives accurate solutions in both high and low Reynolds number flow simulations. The principle of the present RKDG method in the construction of the viscous numerical flux is similar to that of the DG-BGK method but with some significant simplification. The RKDG method uses Runge-Kutta or TVD-RK Shu and Osher (1989) method for the temporal discretization and the DG-BGK method integrates the viscous flow equations in time directly. The RKDG method simulates the viscous flows more accurately than the DG-BGK method as demonstrated by the numerical tests.

2. Runge-kutta discontinuous galerkin method

2.1 RKDG method based on gas-kinetic framework

In the RKDG method Cockburn (2001), a high-order approximate solution inside a cell is updated automatically and limited carefully to enforce the stability and suppress the numerical oscillations. In this section, we will present the RKDG method for the Navier-Stokes equations by incorporating the gas-kinetic formulation.

For a 1D flow, the BGK model in the x-direction is Bhatnagar et al. (1954):

$$f_t + uf_x = \frac{g-f}{\tau} \tag{1}$$

where u is the particle velocity, f is the gas distribution function, and g is the equilibrium state approached by f. The particle collision time τ is related to the viscosity and heat conduction coefficients. The equilibrium state is a Maxwellian distribution,

$$g = \rho(\frac{\lambda}{\pi})^{\frac{K+1}{2}} e^{-\lambda[(u-U)^2+\xi^2]} \tag{2}$$

where ρ is the density, U is the macroscopic velocity, and λ is related to the gas temperature T by $\lambda = m/2kT$, where m is the molecular mass, and K is the Boltzmann constant. The total number of degree of freedom K in ξ is equal to $(5-3\gamma)/(\gamma-1)+2$. In the above equilibrium state g, ξ^2 is equal to $\xi^2 = \xi_1^2 + \xi_2^2 + \cdots + \xi_K^2$. The relation between the macroscopic variables and the microscopic distribution functions is

$$W = (\rho, \rho U, \rho E)^T = \int \phi f du d\xi = \int \phi g du d\xi \tag{3}$$

where ϕ is the vector of moments $\phi = (1, u, (u^2+\xi^2)/2)^T$. Based on the above BGK model, the corresponding Navier-Stokes equations can be derived by Chapman-Enskog expansion up to the first order of τ.

For 1D Navier-Stokes equations $W_t + G_x = 0$, where $G = \int u\phi f du d\xi$, if we express the approximate solution $W^h(x,t)$ as

$$W^h(x,t) = \sum_{l=0}^{k} W_i^l(t)\phi_i^l(x), \quad for \quad x \in I_i, \tag{4}$$

then we can get the following system by a Galerkin method:

$$\frac{d}{dt}W_i^l(t) + \frac{2l+1}{\Delta x_i}(\hat{G}_{i+1/2} - (-1)^l \hat{G}_{i-1/2}) = \frac{2l+1}{\Delta x_i}\int_{I_i} G(x,t)\frac{d}{dt}(\phi_i^l(x))dx. \tag{5}$$

In the following, we will denote the method by the P^k scheme if the approximate solution is approximated by a k th-order polynomial. In order to construct a simple formula of the numerical flux for the RKDG method, we consider the hybridization of the loss and gain terms in a gas distribution function in the present work. As shown in Xu (1998), for the Navier-Stokes solutions the distribution function at

the cell interface can be constructed as

$$f = [1-\eta]f_0 + \eta f_c \tag{6}$$

where f_0 is the initial distribution function, which is also the so-called kinetic flux-vector splitting Navier-Stokes (KFVS-NS) distribution function Chou and Baganoff (1977). f_c is the distribution function due to the collision effect, and η is the relaxation parameter to determine the speed that a system evolves into an equilibrium state and should be a function of local flow variables. In this paper, we construct η as

$$\eta = \exp[-C\frac{|p^l_{i+1/2} - p^r_{i+1/2}|}{p^l_{i+1/2} + p^r_{i+1/2}}]. \tag{7}$$

where $p^{l,r}_{i+1/2}$ are the left and right values of pressure p at the cell interface $x_{i+1/2}$, C is a problem-dependent positive constant, which ranges from 10^3 to 10^3 in our computation.

In the FV BGK method Xu (2001), the initial macroscopic flow states around the cell interface are reconstructed by the MUSCL-type interpolation. But, for the RKDG method, they are updated inside each cell. In the following, $x_{i+1/2} = 0$ will be used for simplicity. With the initial macroscopic flow states on both sides of a cell interface, to the Navier-Stokes order the initial gas distribution function f_0 is constructed as

$$f_0 = \begin{cases} g^l(1 + a^l x - \tau(a^l u + A^l), & x \le 0, \\ g^r(1 + a^r x - \tau(a^r u + A^r), & x \ge 0, \end{cases} \tag{8}$$

where g^l and g^r are the equilibrium states at the left and right hand sides of the cell interface. The distribution function f_c due to the collision effect can be constructed as

$$f_c = g_0[1 - \tau(u\bar{a}^l H[u] + u\bar{a}^r(1 - H[u]) + \bar{A})] \tag{9}$$

where $H[u]$ is the Heaviside function, and g_0 is a local Maxwellian distribution function located at $x = 0$. The calculation of the parameters $a^{l,r}, A^{l,r}$ in f_0 and $\bar{a}^{l,r}$, $\bar{A}$ in g_0 is similar to that in Xu (2001), we omit the details to save space here.

For the Navier-Stokes solutions, the viscosity and heat conduction coefficients are related to the particle collision time τ. With the given dynamical viscosity coefficient μ, the collision time can be calculated by $\tau = \mu / p$, where p is the pressure. Up to this point, we have determined all parameters in the distribution functions f_0 and f_c. After substituting Eqs. (7), (8) and (9) into Eq. (6), we can get the gas distribution function f at the cell interface, then the numerical flux can be obtained by taking the moments $u\phi$ to it. In order to get the heat conduction correct, the energy flux in Eq. (6) can be modified according to the realistic Prandtl number Xu (2001).

The present RKDG method can be easily extended to multidimensional cases. There are two approaches that can be used to construct the numerical flux: one is the directional splitting method Xu (2001) and the other is the fully multidimensional method Xu (2005). In this paper we employ the less costly splitting method to construct the flux at the cell interfaces for efficiency and simplicity consideration. The procedure is similar to 1D case and we omit the details here.

2.2 Limiting procedure and boundary conditions

For the compressible flow simulations by the RKDG method, the direct update of the numerical solution will generate numerical oscillations across strong shock waves. In order to eliminate these oscillations, the non-linear limiter, usually used in the FV method, has to be used in the RKDG method as well. In this paper, in 1D case, we use the Hermite WENO limiter Qiu and Shu (2004) proposed by Qiu and Shu recently. In 2D case, for the rectangular elements a similar limiting procedure to that in Cockburn (1998) is employed. For both 1D and 2D cases, the componentwise limiting operator is used after each Runge-Kutta or TVD-RK Shu and Osher (1989) inner stage.

Now we describe the treatment of boundary conditions. For the adiabatic wall, the no-slip boundary condition for the velocity field is imposed by reversing the velocities in the ghost cell from the sate in the internal region, and the mass and energy densities are put to be symmetric around the wall Xu (2001). For the isothermal wall, where the boundary temperature is fixed, we use the condition of no net mass flux transport across the boundary Xu (2001) to construct the flow states in the ghost cell, and their spacial derivatives are calculated from the data around the wall by appropriate approximation consistent with the accuracy requirement, for example the parabolic reconstruction with the flow states around the wall is used for P^2 scheme. At the inflow/outflow boundaries, the flow states at the external boundary are

computed from the available data and Riemann invariants, the spacial derivatives there are also obtained by appropriate approximation with the given boundary condition.

3. Numerical experiments

The present RKDG method will be tested in both 1D and 2D problems. We use the two-stage TVD-RK time stepping method Shu and Osher (1989) for P^1 case and the three-stage one for both P^2 and P^3 cases, the CFL number is 0.2 for P^1 case and 0.15 for P^2 case.

3.1 Accuracy test

The first test is to solve the Navier-Stokes equations with the following initial data,

$$\rho(x,0)=1+0.2\sin(\pi x),\ U(x,0)=1,\ p(x,0)=1 \quad (10)$$

The dynamical viscosity coefficient is taken as $\mu=0.0005$. The Prandtl number is $\Pr=2/3$ and the specific heat ratio is $\gamma=5/3$. The computational domain is $x\in[0,2]$ and the periodic boundary condition is used. We compute the viscous solution up to time $t=2$ with a small time step to guarantee that the spatial discretization error dominates. No limiter is used in this case. Since there is no exact solution for this problem, we evaluate the numerical error between the solutions by two successively refined meshes and use the error to estimate the numerical convergence rates. The results are shown in Tables 1-3. From these results we can easily see that a $(k+1)$th-order convergence rate can be obtained for $P^k(k=1,2,3)$ case for smooth enough solutions.

Table 1. The error and convergence order for P^1 case.

N	L^∞-error	Order	L^1-error	Order	L^2-error	Order
10	3.05E-2	–	1.76E-2	–	1.99E-2	–
20	5.68E-3	2.42	3.36E-3	2.39	3.79E-3	2.39
40	1.03E-3	2.46	6.31E-4	2.41	7.07E-4	2.42
80	2.08E-4	2.31	1.28E-4	2.30	1.44E-4	2.30

Table 2. The error and convergence order for P^2 case.

N	L^∞-error	Order	L^1-error	Order	L^2-error	Order
10	2.48E-3	–	1.51E-3	–	1.62E-3	–
20	2.76E-4	3.16	1.66E-4	3.18	1.86E-4	3.12
40	2.50E-5	3.47	1.54E-5	3.43	1.73E-5	3.42
80	2.54E-6	3.30	1.47E-6	3.39	1.64E-6	3.40

Table 3. The error and convergence order for P^3 case.

N	L^∞-error	Order	L^1-error	Order	L^2-error	Order
10	9.05E-5	–	5.37E-5	–	5.67E-5	–
20	8.89E-6	3.35	4.23E-6	3.67	4.90E-6	3.53
40	4.90E-7	4.18	2.81E-7	3.91	3.17E-7	3.95
80	3.26E-8	3.91	1.42E-8	4.30	1.70E-8	4.22

3.2 Couette flow

The Couette flow with a temperature gradient provides a good test for the RKDG method to describe the viscous heat-conducting flow. With the bottom wall fixed, the top boundary is moving at a speed U in the horizontal direction. The temperatures at the bottom and top are fixed with values T_0 and T_1. Under the assumption of constant viscosity and heat conduction coefficients and in the incompressible limit, a steady state analytical temperature distribution can be obtained,

$$\frac{T-T_0}{T_1-T_0}=\frac{y}{h}+\frac{\Pr Ec}{2}\frac{y}{H}(1-\frac{y}{H}), \quad (11)$$

where H is the height of the channel, Pr is the Prandtl number, Ec is the Eckert number $Ec=U^2/[C_p(T_1-T_0)]$, and C_p is the specific heat at constant pressure. The results without limiter are shown in Figs. 1-2. From these figures, we see that the numerical results recover the analytical solutions very well with the variations of all these parameters, and the Prandtl number fix does modify the heat conduction term correctly. It is also clearly shown that the higher-order P^2 scheme gives more accurate solutions than the lower-order P^1 scheme with the same mesh size. If we further refine the mesh, the difference between the numerical solution from P^1 and P^2 cases is indistinguishable and both accurately recover the analytical solution.

3.3 Navier-Stokes shock structure

The test is the Navier-Stokes shock structure calculation. Although it is well known that in the high Mach number case the Navier-Stokes solutions do not give the physically realistic shock wave profile, it is still a useful case in establishing and testing a valid solver for the Navier-Stokes equations. The shock structure calculated is for a monotonic gas with $\gamma=5/3$ and a dynamical viscosity coefficient $\mu\sim T^{0.8}$, where T is the temperature. The upstream Mach number M=1.5 and the Prandtl number Pr = 2/3 are used in this test. The dynamical viscosity coefficient at the upstream keeps a constant value

$\mu_{-\infty} = 0.0005$. The results calculated by the second-order P^1 case are presented in Fig. 3 and those by the third-order P^2 case are shown in Fig. 4. From these results, we can see that the shock structure is calculated accurately with a reasonable number of grid points inside the shock layer. Moreover, the third-order scheme gives more accurate results than the second-order scheme, especially in the normal stress and heat flux solutions.

3.4 Laminar boundary layer

The next numerical example is the laminar boundary layer over a flat plate with the length L. The mach number is M=0.2 and the Reynolds number based on the upstream flow states and the length L is $\mathrm{Re} = 10^5$. A non-uniform rectangular mesh with 120×30 cells is used, see Fig. 5. We have compared the numerical results with the theoretical ones given by the well-known Blasius formulae in case of incompressible flow. The U velocity distributions along three different vertical lines are shown in Fig.6. From these figures, we can see that the numerical solutions by both P^1 and P^2 schemes recover the theoretical solution accurately, even with a few grid points in the boundary layer.

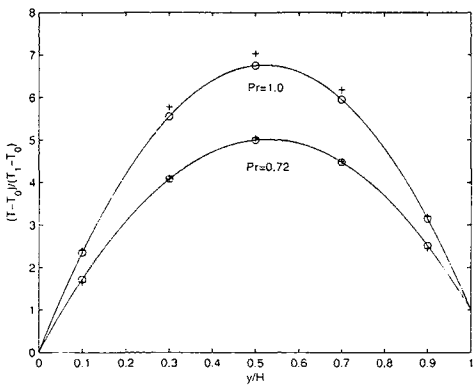

Fig. 1. Couette flow, $\gamma = 5/3, Ec = 50$, '+'-- P^1 case, 'o'-- P^2 case.

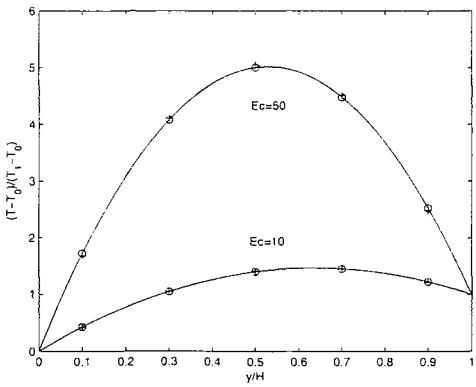

Fig. 2. Couette flow, $\gamma = 1.4, \mathrm{Pr} = 0.72$, '+'-- P^1 case, 'o'-- P^2 case.

3.5 Shock boundary layer interaction

The final test deals with the interaction of an oblique shock with a laminar boundary layer. The shock makes a 32.6^0 angle with the wall, which is located at y=0 and $x \geq 0$, and hits the boundary layer on the wall at $X_s = 10$. The Mach number of the shock wave is equal to 2 and the Reynolds number based on the upstream flow condition and the characteristic length X_s is equal to 2.96×10^5. The dynamical viscosity μ is computed according to the Sutherland's law for the gas with $\gamma = 1.4$ and Pr=0.72. The pressure contours computed by the P^1 and P^2 schemes are presented in Fig. 7. As expected, the P^2 scheme gives a shaper numerical shock transition than that from P^1 scheme due to the less

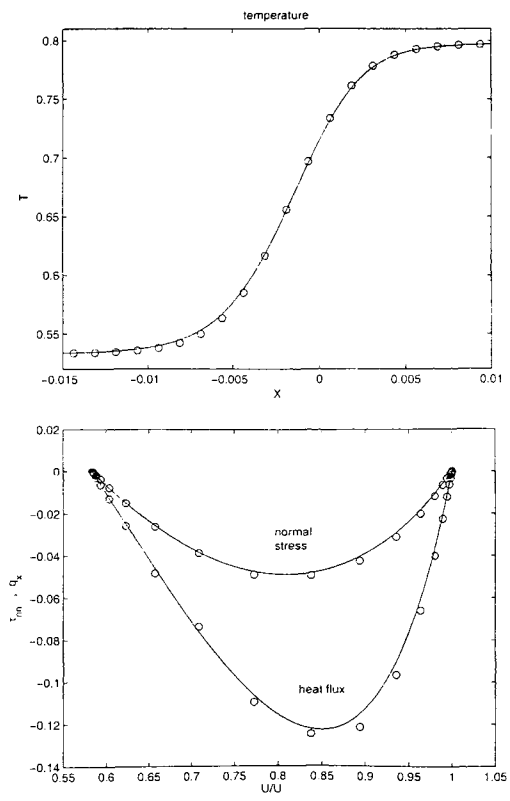

Fig. 3. Navier-Stokes shock structure calculation, P^1 case.

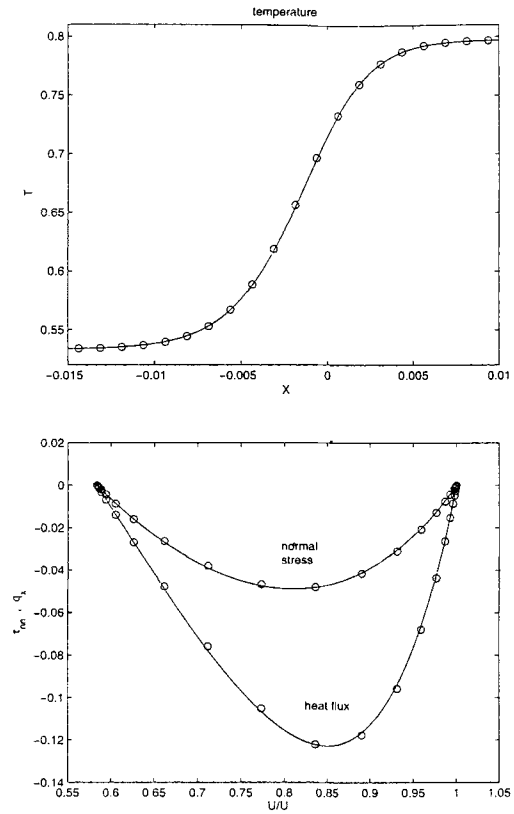

Fig. 4. Navier-Stokes shock structure calculation, P^2 case.

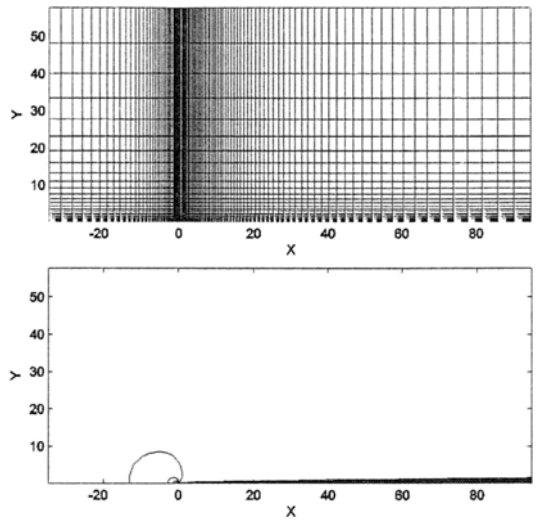

Fig. 5. Mesh(left) and U velocity contours(right) by P^2 case.

numerical dissipation introduced by weaker discontinuities at the cell interfaces. The skin friction and

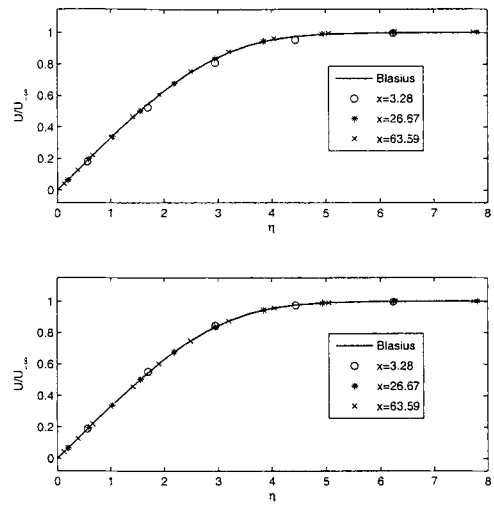

Fig. 6. U velocity distributions along three vertical lines, left P^1, right P^2.

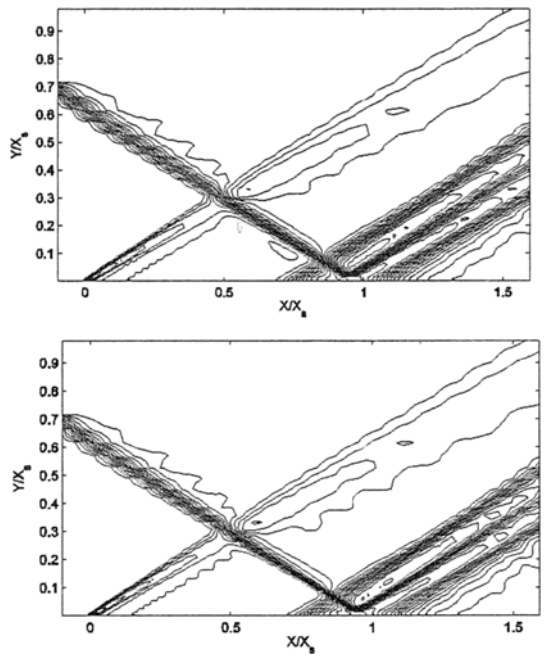

Fig. 7. Shock boundary interaction, 30 equally spaced contours of pressure p/p_{∞} from 0.997 to 1.411 by P^1 (left) and P^2 (right) cases.

pressure distributions at the plate surface are shown in Fig. 8, where a fair agreement with the experimental data Hakkinen et al. (1959) is obtained for both P^1 and P^2 schemes. Our numerical results are comparable with those in Ohwada and Fukata (2006).

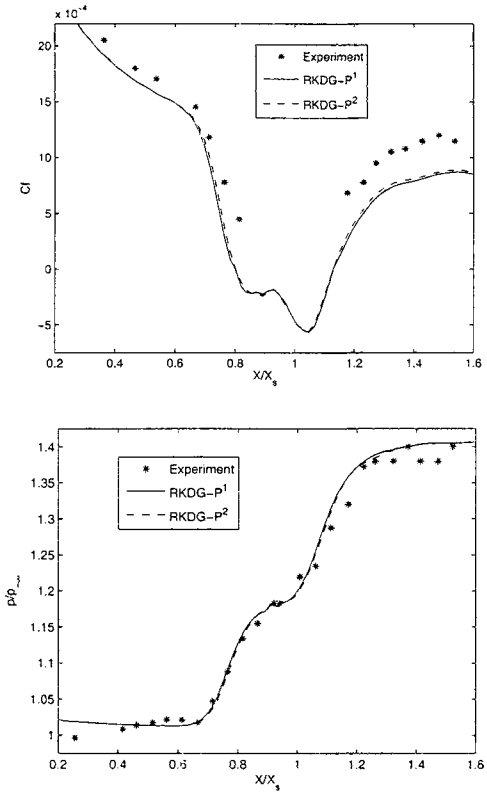

Fig. 8. Shock boundary interaction, skin friction coefficient (left) and pressure (right) distributions at the plate surface.

4 Conclusion

In this paper, a RKDG method for the viscous flow computation has been presented. The construction of the RKDG method is based on a gas-kinetic formulation, which combines the convective and dissipative terms in a single gas distribution function. Due to the intrinsic connection between the gas-kinetic BGK model and the Navier-Stokes equations, the Navier-Stokes flux is automatically obtained by the method. The current RKDG method has good shock capturing capacity, where the numerical dissipation introduced from the numerical flux at the cell interface is controlled adaptively by a hybrid parameter in the current approach. The RKDG method works very well for all test cases presented. The higher-order P^2 scheme does give a more accurate solution than that from the lower-order P^1 scheme, especially in the well-resolved cases. In terms of the computational cost, the present RKDG method is more expensive, especially in the multi-dimensional cases, than the finite volume gas-kinetic BGK method for the Navier-Stokes equations. An implicit version of the DG method is under consideration for the efficiency purpose. Like many other DG methods, for the flow with discontinuities the overall performance of the scheme depends strongly on the limiters used.

Acknowledgement

The work described in this paper was substantially supported by grants from the Research Grants council of the Hong Kong Special Administrative region, China (HKUST621005, 621406)

References

Arnold, D. N., Brezzi, F., Cockburn, B. and Marini, L. D., 2002, "Unified Analysis of Discontinuous Galerkin Methods for Elliptic Problems," *SIAM J. Numer. Anal.* Vol. 39, p. 1749.

Bassi, F. and Rebay, S., 1997, "A High-order Accurate Discontinuous Finite Element Method for the Numerical Solution of the Compressible Navier-Stokes Equations," *J. Comput. Phys.* pp. 131~267.

Baumann, C. E. and Oden, J. T., 1999, "A Discontinuous *hp* Finite Element Method for the Euler and Navier-Stokes Equations," *Int. J. Numer. Methods in Fluids,* Vol. 31, p. 79.

Bhatnagar, P. L., Gross, E. P. and Krook, M., 1954, "A Model for Collision Processes in gases I: Small Amplitude Rocesses in Charged and Neutral One-component Systems," *Phys. Rev.* Vol. 94, p. 511.

Chou, S. Y. and Baganoff, D., 1997, "Kinetic Flux-Vector Splitting for the Navier-Stokes Equations," *Comput. Phys.* Vol. 130, p. 217.

Cockburn, B., Karniadakis, G. E. and Shu, C. W., 2000, "The Development of Discontinuous Galerkin Methods," Discontinuous Galerkin Methods: Theory, Computation and Applications, Springer, Berlin.

Cockburn, B. and Shu, C. W., 1989a, "TVB Runge-Kutta Local Projection Discontinuous Galerkin Finite Element Method for Scalar Conservation Laws II: General framework," *Math. Comp.* Vol. 52, p. 411.

Cockburn, B., Lin, S. Y. and Shu, C. W., 1989b, "TVB Runge-Kutta Local Projection Discontinuous Galerkin Finite Element Method for Conservation Laws III: One Dimensional Systems," *J. Comput. Phys.* Vol. 84, p. 90.

Cockburn, B., Hou S. and Shu, C. W., 1990, "TVB

Runge-Kutta Local Projection Discontinuous Galerkin Finite Element Method for Conservation Laws IV: The Multidimensional Case," *Math. Comp.* Vol. 54, p. 545.

Cockburn, B. and Shu, C. W., 1998, "The Runge-Kutta Discontinuous Galerkin Method for Conservation Laws V: Multidimensional Systems," *J. Comput. Phys.* Vol. 141, p. 199.

Cockburn, B. and Shu, C. W., 1998, "The Local Discontinuous Galerkin Method for Time-Dependent Convection-diffusion Systems," *SIAM J. Numer. Anal.* Vol. 35, p. 2440

Cockburn, B. and Shu, C. W. 2001, "Runge-Kutta Discon-tinuous Galerkin Method for Convection-Dominated Problems," *J. Sci. Comput.* Vol. 16, p. 173.

Hakkinen, R. J., and Greber, L., Trilling, L. and Abarbanel, S. S., 1959, "The Interaction of an Oblique Shock Wave with a Laminar Boundary Layer," *NASA Memo.* 2-18-59W, NASA.

Ohwada, T. , 2002, "On the Construction of Kinetic Schemes," *J. Comput. Phys.* Vol. 177, p. 156.

Ohwada, T. and Fukata, S., "Simple Derivation of High-resolution Schemes for Compressible Flows by Kinetic Approach," *J. Comput. Phys.* Vol. 211, p. 424.

Qiu, J. and Shu, C. W., 2004, "Hermite WENO Schemes and Their Application as Limiters for Runge-Kutta Discontinuous Galerkin Method: One Dimensional Case," *J. Comput. Phys.* Vol. 193, p. 115.

Shu, C. W. and Osher, S., 1989, "Efficient Implementation of Essential Non-oscillatory Shock Capturing-Schemes," *II, J. Comput. Phys.* Vol. 83, p. 32.

Tang, H. Z. and Warnecke, G., 2005, "A Runge-Kutta Discontinuous Galerkin Method for the Euler Equations," *Computers & Fluids,* Vol. 34, p. 375.

van Leer, B., 1977, "Towards the Ultimate Conservative Difference Scheme IV. A New Approach to Numerical Convection," *J. Comput. Phys.* Vol. 23, p. 276.

van Leer, B. and Nomura, S., 2005 "Discontinuous Galerkin for Diffusion," *AIAA-2005-5108, 17th AIAA Computational Fluid Dynamics Conference.*

Xu, K., 1998, "Gas-kinetic Schemes for Unsteady Compressible flow Simulations," *VKI for Fluid Dynamics Lecture Series 1998-03.*

Xu, K., 2001, "A Gas-kinetic BGK Scheme for the Navier-Stokes Equations and Its Connection with Artificial Dissipation and Godunov Method," *J. Comput. Phys.* Vol. 171, p. 289.

Xu, K. and Jameson, A., 1995, "Gas-Kinetic Relaxation (BGK-type) Schemes for the Compressible Euler Equations," *AIAA-95-1736, 12th AIAA Computational Fluid Dynamics Conference.*

Xu, K. and Li, Z. W., 2001, "Dissipative Mechanism in Godunov-type Schemes," *Int. J. Numer. Methods in Fluids*, Vol. 37, p. 1.

Xu, K., Mao, M. L. and Tang, L., "A Multidimensional Gas-kinetic BGK Scheme for Hypersonic Viscous flow," *J. Comput. Phys.* Vol. 203, p. 405.

Xu, K., 2004, "Discontinuous Galerkin BGK Method for Viscous flow Equations: One-Dimensional Systems," *SIAM J. Sci. Comput.* Vol. 23, p. 1941.